

## Three-dimensional mapping reveals scale-dependent dynamics in biogenic reef habitat structure

Jackson-Bué, Tim; Williams, Gareth; Walker-Springett, Guy; Rowlands, Steven; Davies, Andrew

### Remote Sensing in Ecology and Conservation

DOI:  
[10.1002/rse2.213](https://doi.org/10.1002/rse2.213)

Published: 01/12/2021

Publisher's PDF, also known as Version of record

[Cyswllt i'r cyhoeddiad / Link to publication](#)

*Dyfyniad o'r fersiwn a gyhoeddwyd / Citation for published version (APA):*  
Jackson-Bué, T., Williams, G., Walker-Springett, G., Rowlands, S., & Davies, A. (2021). Three-dimensional mapping reveals scale-dependent dynamics in biogenic reef habitat structure. *Remote Sensing in Ecology and Conservation*, 7(4), 621-637. <https://doi.org/10.1002/rse2.213>

#### Hawliau Cyffredinol / General rights

Copyright and moral rights for the publications made accessible in the public portal are retained by the authors and/or other copyright owners and it is a condition of accessing publications that users recognise and abide by the legal requirements associated with these rights.

- Users may download and print one copy of any publication from the public portal for the purpose of private study or research.
- You may not further distribute the material or use it for any profit-making activity or commercial gain
- You may freely distribute the URL identifying the publication in the public portal ?

#### Take down policy

If you believe that this document breaches copyright please contact us providing details, and we will remove access to the work immediately and investigate your claim.

## ORIGINAL RESEARCH

# Three-dimensional mapping reveals scale-dependent dynamics in biogenic reef habitat structure

Tim Jackson-Bu  <sup>1</sup> , Gareth J. Williams<sup>1</sup> , Guy Walker-Springett<sup>1</sup> , Steven J. Rowlands<sup>1</sup>  & Andrew J. Davies<sup>2</sup> 

<sup>1</sup>School of Ocean Sciences, Bangor University, Menai Bridge Isle of Anglesey, LL59 5AB, UK

<sup>2</sup>Department of Biological Sciences, University of Rhode Island, Kingston Rhode Island, 02881, USA

## Keywords

Autocorrelation, ecosystem dynamics, reef accretion, reef erosion, reef mapping, spatial ecology

## Correspondence

Tim Jackson-Bu  , School of Ocean Sciences, Bangor University, Menai Bridge, Isle of Anglesey LL59 5AB, UK. Tel: +44 (0) 7841463590; Fax: +44 (0) 1248716729; E-mail: tim.jackson-bue@bangor.ac.uk

Editor: Kylie Scales  
Associate Editor: Vincent Lecours

Received: 29 January 2021; Revised: 26 April 2021; Accepted: 28 April 2021

doi: 10.1002/rse2.213

*Remote Sensing in Ecology and Conservation* 2021;7 (4):621–637

## Abstract

Habitat structure influences a broad range of ecological interactions and ecosystem functions across biomes. To understand and effectively manage dynamic ecosystems, we need detailed information about habitat properties and how they vary across spatial and temporal scales. Measuring and monitoring variation in three-dimensional (3D) habitat structure has traditionally been challenging, despite recognition of its importance to ecological processes. Modern 3D mapping technologies present opportunities to characterize spatial and temporal variation in habitat structure at a range of ecologically relevant scales. Biogenic reefs are structurally complex and dynamic habitats, in which structure has a pivotal influence on ecosystem biodiversity, function and resilience. For the first time, we characterized spatial and temporal dynamics in the 3D structure of intertidal *Sabellaria alveolata* biogenic reef across scales. We used drone-derived structure-from-motion photogrammetry and terrestrial laser scanning to characterize reef structural variation at mm-to-cm resolutions at a habitat scale (~35 000 m<sup>2</sup>) over 1 year, and at a plot scale (2500 m<sup>2</sup>) over 5 years (2014–2019, 6-month intervals). We found that most of the variation in reef emergence above the substrate, accretion rate and erosion rate was explained by a combination of systematic trends with shore height and positive spatial autocorrelation up to the scale of colonies (1.5 m) or small patches (up to 4 m). We identified previously undocumented temporal patterns in intertidal *S. alveolata* reef accretion and erosion, specifically groups of rapidly accreting, short-lived colonies and slow-accreting, long-lived colonies. We showed that these highly dynamic colony-scale structural changes compensate for each other, resulting in seemingly stable reef habitat structure over larger spatial and temporal scales. These patterns could only be detected with the use of modern 3D mapping technologies, demonstrating their potential to enhance our understanding of ecosystem dynamics across scales.

## Introduction

Ecosystems are dynamic (Odum, 1969). Gradients in biophysical and human socioeconomic drivers create complex mosaics in ecosystem properties (Legendre & Fortin, 1989; Perry, 2002; Williams et al., 2019), with the patterns we observe determined by the scale of our observations (Levin, 1992; Wiens, 1989). Because ecosystem patterns and processes are intrinsically linked, we can gain a deeper understanding about ecological processes and their

drivers by quantifying these underlying patterns across scales (Horne & Schneider, 1995; Underwood et al., 2000). Quantifying patterns in ecosystem properties not only advances ecological insight, but also facilitates evidence-based management by enabling us to detect change in ecosystem characteristics like habitat structure in response to disturbance (Landres et al., 1999).

Physical habitat structure can be abiotic like rocks on a shoreline, or biogenic like the trees of a forest. These features determine habitat structural complexity and influence

the biodiversity and community composition of associated ecological communities through myriad processes. These include buffering organisms from extreme environmental conditions (Scheffers et al., 2014), mediating resource availability (Safriel & Ben-Eliahu, 1991) and providing shelter for prey species from predation (Stevenson et al., 2015; Warfe et al., 2008). Biogenic reefs are complex habitats in which substrate and structure is generated and amplified by engineering organisms (Jones et al., 1994). Biogenic reefs represent global biodiversity hotspots and provide a range of ecosystem services to humanity (Bruschetti, 2019; Connell, 1978; Dubois et al., 2002; Woodhead et al., 2019). Spatially and temporally dynamic three-dimensional (3D) structure is critical to the biodiversity, ecological functioning and conservation value of biogenic reefs (Graham & Nash, 2013; Holt et al., 1998). Metrics of reef structure can also be an indicator of the health of the engineering species (Curd et al., 2019) and reef recovery potential following acute disturbance (Graham et al., 2015). To understand organism–habitat interactions within biogenic reef systems, we must first identify the patterns and scales of variation inherent within their structures (Holt et al., 1998; Jenkins et al., 2018).

Much of our understanding about scale-dependent processes in ecosystems derives from terrestrial landscape ecology. The study of spatial patterns in terrestrial systems has greatly benefitted from remote sensing, providing high-resolution spatially continuous data for a variety of ecosystem properties including 3D habitat structure (Chambers et al., 2007; Vierling et al., 2008). Remote sensing of 3D structure in the marine environment from satellite or crewed aircraft improves ecological insight in clear, shallow waters (Wedding et al., 2019), but similar information is challenging and expensive to capture in deep or turbid waters (Lecours et al., 2015). Recent developments in high-resolution 3D mapping technologies including structure-from-motion photogrammetry and laser scanning offer the potential to study patterns in 3D structure from organism to habitat scales, and are practical for investigation of scale-dependent properties in marine and coastal habitats (Calders et al., 2020; Urbina-Barreto et al., 2021). This creates opportunities to apply conceptual and analytical frameworks from landscape ecology, such as identification of dominant spatial scales of variation (Legendre & Fortin, 1989), at new scales and in new systems. The ability to record spatially continuous 3D habitat structure across km extents at mm resolution, with rapid repeats and low operating costs is sparking a revolution in the scope and scale of ecological investigations (D'Urban Jackson et al., 2020).

Here, we use intertidal habitat structure built by *Sabellaria alveolata*, a reef-building annelid, as a model system to characterize scale-dependent structural dynamics in

complex biogenic reef habitats using high-resolution 3D mapping. *S. alveolata* reef comprises colonies of sediment tubes biocemented together, creating extensive reefs on northeast Atlantic and Mediterranean coasts (Bruschetti, 2019; Godet et al., 2011; La Porta & Nicoletti, 2009). Similar reefs built by other species in the Sabelliidae family are found globally (Capa et al., 2012). Our current understanding of the scale-dependent structural dynamics in biogenic reefs is hampered by a lack of spatio-temporal information about habitat structure across scales. To explore this, we quantify spatial and temporal patterns in reef structure at mm-to-cm resolution, at plot- (2500 m<sup>2</sup>) to habitat-scale (~35 000 m<sup>2</sup>) extents and over temporal scales of 1–5 years. Our findings reveal previously undescribed patterns of structural variation in intertidal biogenic reefs and demonstrate the enhanced ecological insight gained from the application of modern remote-sensing technologies for 3D ecosystem mapping in structurally complex habitats.

## Materials and Methods

### Data collection

#### Study site

To characterize variation in biogenic reef habitat structure across scales, we conducted high-resolution 3D mapping at a *Sabellaria alveolata* reef habitat at Llanddulas, Wales, UK (53.294 N, 3.632 W), using two techniques between 2014 and 2019 (Fig. 1). The reef at Llanddulas occupies the low shore for at least 1 km along a moderately exposed, unconsolidated cobble beach with a gentle slope gradient of 3%.

#### Plot-scale (2500 m<sup>2</sup>) 3D mapping

We collected data to investigate multi-annual temporal patterns in *S. alveolata* reef structure using terrestrial laser scanning (HDS ScanStation C10, Leica Geosystems, Switzerland) of a permanent 2500 m<sup>2</sup> reef plot at c. 6-month intervals (autumn and spring) over 5 years from September 2014 to October 2019. Terrestrial laser scanning generates high-resolution (thousands of points per m<sup>2</sup>) data with mm precision and was the most advanced 3D mapping technology available for field sampling at the start of the study in 2014. We conducted medium-resolution (0.1 m point spacing at 100 m range) scans of the plot from several stationary positions per time point, ensuring similar data coverage among time points. We used retro-reflective sphere reference targets to align scan datasets within a time point. Aligning datasets from different time points typically uses global navigation satellite system (GNSS) georeferencing or permanent reference targets. Our

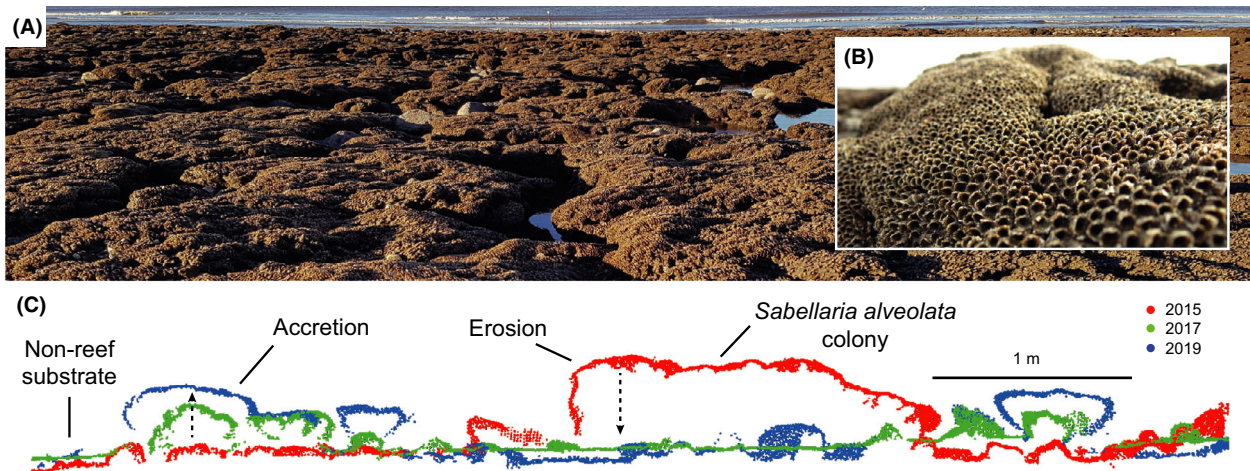


**Figure 1.** (A) *Sabellaria alveolata* biogenic reef habitat comprises aggregations of sediment tubes in colonies that emerge above a hard, non-reef substrate. (B) Close-up image of a prograding colony surface showing dense tube openings of ~5 mm diameter. (C) Cross section of 3D terrestrial laser scan point cloud data from 3 years, demonstrating the detailed information about spatial and temporal dynamics in habitat structure that can be captured using modern 3D mapping technology. Reef colonies accrete upwards and outwards from the non-reef substrate in characteristic mushroom-like hummocks that coalesce into platforms. Erosion of reef colonies is often rapid and catastrophic.

plot was intertidal with an unconsolidated substrate, so permanent targets could not be left and expected not to move, and alignment by GNSS georeferencing would have introduced error on the same scale (cm) as the changes we expected to detect, limiting their reliable detection and interpretation. Therefore, to enable accurate alignment of repeat surveys, we increased the laser scanning data coverage to include permanent nearby features (rock groynes, cycle path and buildings), enabling us to align the datasets using the geometry of these stable features, without constraining the data across the dynamic foreshore.

We quality checked, aligned, georeferenced and manually cleaned the laser scanning point cloud data in Cyclone v9 software (Leica Geosystems, Switzerland). Within a time point, we aligned datasets from different scanner positions to 6 mm accuracy using target positions. We then aligned complete datasets from different time points to 6 mm accuracy using the geometry of permanent features. We made a final adjustment to the vertical alignment within the plot based on stable regions of non-reef substrate. We standardized datasets from different time points by cropping to the plot extent, subsampling point clouds to a minimum point spacing of 5 mm, and removing isolated points using the *statistical outlier removal* tool in the open source software CloudCompare v2.11 (CloudCompare, 2019).

### Habitat-scale (~35 000 m<sup>2</sup>) 3D mapping

Terrestrial laser scanning was impractical for the larger extent of habitat-scale sampling within short low-tide

windows. Therefore, to investigate spatial and temporal patterns in *S. alveolata* reef structure at a habitat scale (~35 000 m<sup>2</sup>), we used structure-from-motion photogrammetry derived from drone aerial imagery, in April 2018 and April 2019. Drone-derived structure-from-motion photogrammetry generates continuous 3D information across large extents, with comparable accuracy to terrestrial laser scanning in complex habitats like *S. alveolata* reef (D'Urban Jackson et al., 2020). We used a Phantom 4 Pro (DJI) with a 20 MP camera flying at 46 m altitude to capture images with 14-mm XY ground resolution, covering c. 150 000 m<sup>2</sup> of the coastline. The flight pattern was pre-determined and flying was automated using software (Maps Made Easy) to ensure the same survey pattern was flown in both years. To optimize the 3D modelling process, we used a high image overlap, so that every XY position in the area of interest was captured in at least five images. We generated 3D models for each survey using the industry standard software Pix4Dmapper Pro v4. Unlike terrestrial laser scanning, for structure-from-motion photogrammetry, we required georeferenced ground control points to scale, constrain and align the 3D models. We used 11 (2018) and 19 (2019) control points surveyed with commercial GNSS equipment (system 1200, Leica Geosystems, Switzerland), giving root mean square errors of 9 and 32 mm respectively. Because there were no permanent features within the study area, we verified vertical alignment accuracy by calculating elevation difference at 100 random points along a cycle path adjacent to the study area, giving a median difference of 23 mm and root mean square error of 26 mm. This

represents a worst-case estimate because the cycle path was outside the area constrained by control points. From the 3D models and aerial images, we generated digital surface models (DSMs, 0.1 m XY resolution) and orthomosaics (0.02 m XY resolution) for 2018 and 2019.

## Data analysis

### Habitat-scale (~35 000 m<sup>2</sup>) spatial patterns in *S. alveolata* reef emergence, accretion rate and erosion rate

To study habitat-scale spatial patterns of variation in *S. alveolata* reef structure, we conducted variography (Fig. 2, Data S1) using the drone-derived DSMs from 2018 and 2019. To investigate reef structure independently from trends in the underlying non-reef substrate, we calculated reef *emergence*, defined as the height of the DSM surfaces above a standardized digital elevation model (DEM) representing the lowest levels in the non-reef substrate (Fig. 3). We used a threshold of emergence to classify DSM cells as reef ( $\geq 0.15$  m) or non-reef substrate ( $< 0.15$  m) within a reef area polygon (36 363 m<sup>2</sup>) digitized from the 2018

orthomosaic (Fig. 5A). We validated the classification by manually classifying 500 random points on the orthomosaic and interpreting a confusion matrix of predicted against observed classes. Overall accuracy (correct predictions out of total predictions) was 81.2%, precisions (true positives out of total positive predictions) were 91.7 and 80.1% for reef and non-reef substrate respectively. To study spatial patterns in accretion (positive change) and erosion (negative change) of *S. alveolata* reef, we calculated the vertical difference between the DSMs from April 2018 and April 2019 to provide accretion and erosion rates as positive and negative vertical change per year.

To characterize spatial variation in habitat-scale *S. alveolata* reef structure, we modelled trends and conducted variography using emergence, accretion rate and erosion rate values of the 9140 reef cells in a random sample of 100 000 cells in the reef area. Our data exploration indicated that emergence, accretion rate and erosion rate had trends with shore height and along-shore distance and were anisotropic with a major axis along the shore and minor axis down the shore. To meet the Gaussian distribution requirements of linear modelling and variography, we transformed the data using ordered quantile

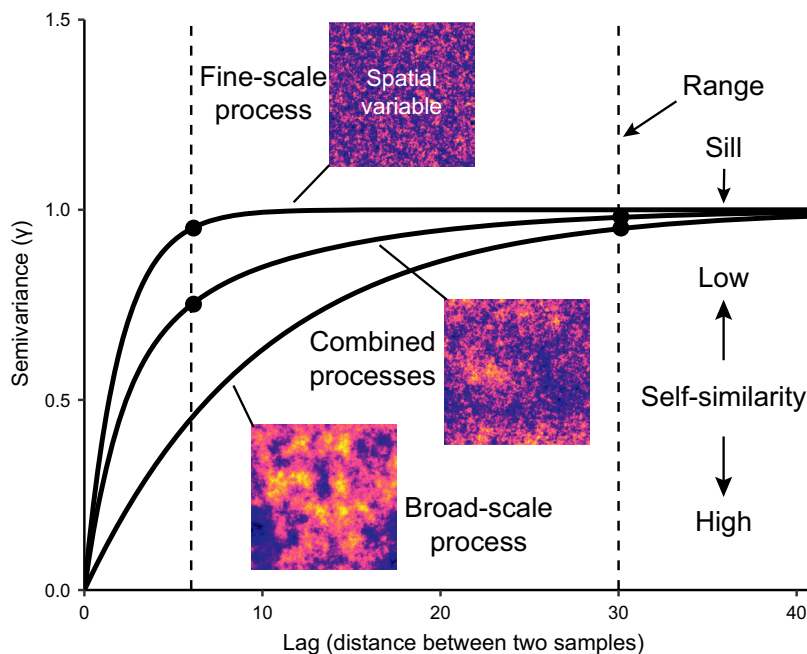


**Figure 2.** Interpreting spatial patterns in processes that generate spatial variables using variography. Variograms visualize spatial self-similarity, or autocorrelation, in a variable by plotting semivariance ( $\gamma$ ) against lag, the distance between two samples. As lag increases samples become less similar (higher  $\gamma$ ) until a plateau (sill) is reached at a distance (range), beyond which sample values are not autocorrelated. Here we show three simulated examples of a variable generated with different processes, and their respective variograms. Top: a fine-scale process generates a variable that is autocorrelated only over short distances, so the range (point and dashed line) is small. Bottom: a broad-scale process generates a variable that is autocorrelated over longer distances, producing a variogram with a larger range. Middle: the fine- and broad- scale processes have been added together, producing a variable with both short- and long-distance autocorrelation, generating a nested variogram with two ranges.

transformation (Peterson & Cavanaugh, 2020), then modelled trends using ordinary least squares linear regression. We conducted variography on the linear model residuals along two axes: along the shore ( $120^\circ$  from north) and down the shore ( $30^\circ$  from north), with maximum lags of 250 and 50 m, respectively, approximately two thirds of the maximum reef area dimensions, using the *gstat* package in R (Graler et al., 2016; Pebesma, 2004; R Core Team, 2020). We fitted an initial variogram model to each experimental variogram automatically, then improved the fit by adjusting the model parameters and adding a secondary variogram model where appropriate, until a visual good fit was found to the experimental variogram (Gringarten & Deutsch, 2001). To investigate whether patterns in reef structure were related directly to patterns in the underlying non-reef substrate topography, we conducted variography using emergence data from 10 000 random non-reef substrate DSM cells.

The trend in mean emergence with shore height explained only a small amount of the variation ( $R^2 = 0.043$ , Table S1). Our data exploration showed that the reef comprised colonies at all stages of emergence, from the classification threshold of 0.15 m up to an emergence limit that was related to shore height. Therefore, shore height appeared to represent a limiting factor and so maximum emergence was a better metric for characterizing habitat structure than a measure of central tendency (Kaiser et al., 1994). To examine the relationship between maximum reef emergence and shore height, we used a sample of 2000 reef cells with a minimum point spacing of 1.5 m derived from the variography results, 1.5 m being the dominant range of spatial autocorrelation. We modelled the relationship between maximum (99<sup>th</sup> percentile) reef emergence and DEM elevation with linear quantile regression, using the *quantreg* package in R (Koenker, 2020).

### Plot-scale (2500 m<sup>2</sup>) temporal patterns in reef structure

To characterize multi-annual structural changes in *S. alveolata* reef structure, we used terrestrial laser scanning to survey a 2500 m<sup>2</sup> plot in autumn and spring from September 2014 to October 2019. To track vertical changes in reef emergence through time, we digitally sampled locations within the plot ( $n = 454$ ) that had reef presence in at least one time point, avoided reef colony edges where lateral accretion and erosion would confuse interpretation, and were spatially independent (Fig. 4, Data S2). At each sample location and for each time point, we extracted mean emergence above a common DEM. To examine common characteristics in temporal changes in reef emergence, we derived accretion

and emergence metrics from each sample time series. We calculated mean and maximum annual accretion rate, maximum emergence and time spent within 80% of maximum emergence, which we termed *persistence*. We then used partitioning around medoids (PAM) clustering, a common data clustering method that is robust to outliers (Kaufman & Rousseeuw, 1990), to classify sample time series into two groups with similar metrics using the *cluster* package in R (Maechler et al., 2019).

Following evidence of multiannual cycles of habitat-scale accretion and erosion (Gruet, 1986), we hypothesized that mean plot-scale reef emergence would vary over the 5-year study period. We also hypothesized that due to higher productivity in summer and lower growth rates coupled with more destructive wave action in winter, plot-scale emergence would be higher in autumn than in spring. We tested these hypotheses using a two fixed-factor (year and season) permutational analysis of variance (Anderson, 2001) with reef emergence as a univariate response. The permutational nature of the test removes the need to satisfy normality in the response variable as the routine permutes the raw data to generate the null distribution (Anderson, 2001). To ensure a balanced design with no missing data and no repeat sampling, we first divided reef sample locations ( $n = 454$ ) randomly and equally among season (two levels: autumn and spring) and year (five levels: 2015–2019) combinations (10 combinations,  $n = 45$ ). Some reef sample locations contained missing data for certain season and year combinations, so we iteratively exchanged these reef sample locations among groups until no missing data remained. Homogeneity of variance between factor levels was confirmed with Levene's test ( $P > 0.05$ ). Our permutational analysis of variance was based on a Euclidean distance similarity matrix of the raw reef emergence data, with 9999 random permutations under a reduced model and Type III (partial) sums of squares. Where there was global model significance, permutational pairwise tests were used to determine where the differences occurred between factor levels.

## Results

### Habitat-scale (~35 000 m<sup>2</sup>) spatial patterns in *S. alveolata* reef emergence, accretion rate and erosion rate

We estimated the percentage cover of *S. alveolata* reef within the 36 363 m<sup>2</sup> reef area as 26.8% or a total coverage of 9745 m<sup>2</sup> based on our binary classification of the 0.1-m XY-resolution emergence raster into reef or non-reef substrate (Fig. 5A). Maximum reef emergence (99<sup>th</sup>

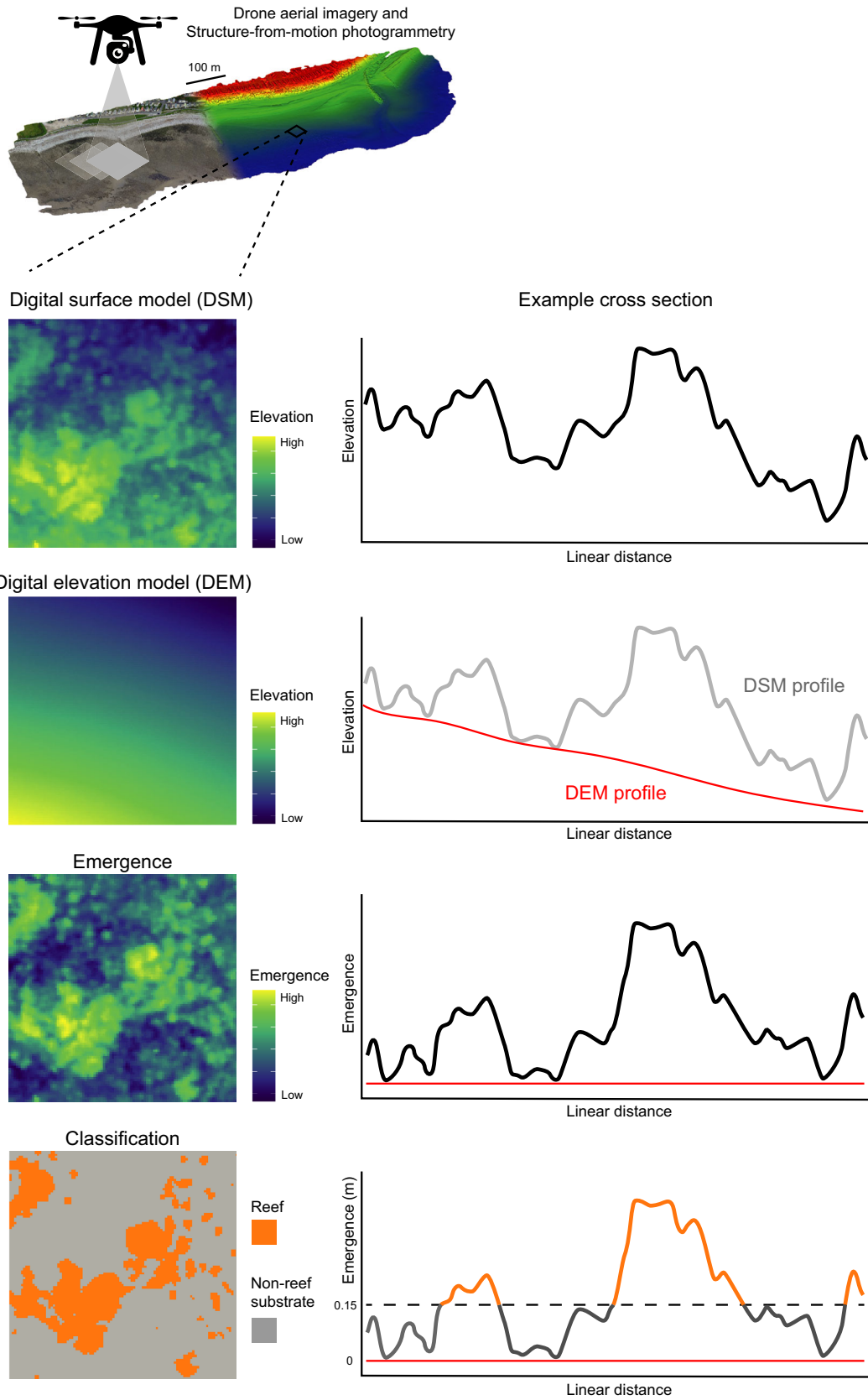


**Figure 3.** Data processing method used to classify habitat-scale digital surface models (DSMs) as reef or non-reef substrate. We generated 0.1 m XY resolution DSMs using drone aerial imagery and structure-from-motion photogrammetry. From the DSM we generated a digital elevation model (DEM) representing the ground level at the same resolution by interpolating between the lowest point in each square of a 2 m grid. We calculated emergence by subtracting the DEM from the DSM elevation. Finally, within the known reef area (Fig. 5A) we used a binary classification of reef ( $\geq 0.15$  m emergence) and non-reef substrate ( $< 0.15$  m emergence).

percentile) increased down the shore from c. 0.2 m at 0 m ordnance datum Newlyn (ODN) to a maximum of 0.5 m above the substrate at 2.8 m below ODN (Fig. 5B). The relationship was described by:

$$\log(\text{emergence}_{\max}) = -0.308(\text{shore height}) - 1.551 \quad (1)$$

Reef emergence was positively spatially autocorrelated up to 1.5 m in both along shore and down shore directions, represented by a spatial structure that described 65–70% of the variance (Fig. 5C, Table S1). There was a smaller amount of residual positive autocorrelation in reef emergence over larger distances along the shore (up to 110 m) and down the shore (up to 20 m) (Fig. 5C, Table S1). At larger distances still, the variogram indicated additional patterns in spatial dependence of reef emergence including cyclicity, but these were not quantified because variogram model fitting becomes less reliable at larger distances relative to the study extent. The variogram of non-reef substrate emergence showed that the dominant autocorrelation pattern mostly occurred over a larger distance of 4.5 m and explained a higher proportion (90%) of the variation compared to reef emergence (Table S1). A small amount of spatial autocorrelation in non-reef substrate emergence was also evident over larger distances (up to 50–90 m).

At the habitat scale ( $\sim 35\,000\text{ m}^2$ ), the elevation of *S. alveolata* reef colonies changed by  $19 \pm 82$  mm (mean  $\pm 1$  SD) between April 2018 and April 2019 (Fig. 6A). The small magnitude of mean elevation change across the total reef area was the result of a balance between variable positive and negative changes in individual samples (0.1-m XY-resolution cells). A high proportion of reef samples (80%) showed a small positive elevation change (accretion,  $49 \pm 30$  mm), with the remaining samples (20%) showing larger and more variable negative changes (erosion,  $-99 \pm 113$  mm). Both accretion and erosion maxima increased towards the lower shore (Fig. 6A) and showed different spatial autocorrelation patterns. Positive spatial autocorrelation in accretion mostly occurred within short distances (up to 0.75–1.05 m), with a small proportion of positive autocorrelation extending over larger distances up to 40–130 m (Fig. 6B, Table S2). In contrast, erosion of reef material was only positively spatially autocorrelated up to distances of 2.9–3.8 m, beyond which the variogram indicated spatial randomness (Fig. 6C, Table S2).

### Plot-scale (2500 m<sup>2</sup>) temporal patterns in reef structure

Within the 2500 m<sup>2</sup> plot, overall reef emergence across all 11 time points over 5 years was  $0.22 \pm 0.13$  m (mean  $\pm 1$  SD). We found scale-dependent variation, with high variation in emergence at each sample location (colony scale,  $n = 454$ ) through time and high variation among samples at each time point, but low variation in plot-scale emergence through time. The coefficient of variation (mean  $\pm 1$  SD) in sample location emergence through time was  $52 \pm 32.3$  and per time point was  $56.5 \pm 3.7$ , whereas the coefficient of variation in plot-scale mean emergence through time was 8.8.

Time series of emergence at reef sample locations revealed diverse temporal patterns in emergence, accretion and erosion metrics of colonies that we classified into two groups called *fast* and *slow* colonies (Fig. 7). These two groups clustered moderately well, indicated by an average silhouette width of 0.35 on a scale from 0 (poorly clustered) to 1 (perfectly clustered) (Kaufman & Rousseeuw, 1990). Fast colonies were characterized by higher maximum and mean annual accretion, higher maximum emergence and shorter persistence (time spent within 80% of their maximum emergence) than slow colonies (Fig. 7, Table S3). Visual assessment showed that slow colonies were evenly distributed throughout the plot, whereas fast colonies were concentrated in the northern, lower-shore half of the plot (Fig. S1). We found that erosion of reef colonies often occurred rapidly in both groups; it was common for emergence to drop to the level of the non-reef substrate within 6 months to a year (Fig. 7).

There was a significant interaction between ‘year’ and ‘season’ on plot-scale reef emergence ( $F_{4,440} = 3.48$ ,  $P = 0.009$ , Table S4) driven entirely by emergence being higher in autumn than spring in 2015 ( $P = 0.001$ ). Across season, there were no differences among years in spring emergence, but there were significant differences in autumn, with 2015, 2016 and 2019 having higher emergence than 2017 and 2018 ( $P < 0.05$ , Fig. S2, Table S4).

## Discussion

Habitat structure strongly dictates ecological function in complex 3D ecosystems. Quantifying how 3D habitat structure varies across space and time is, therefore, a

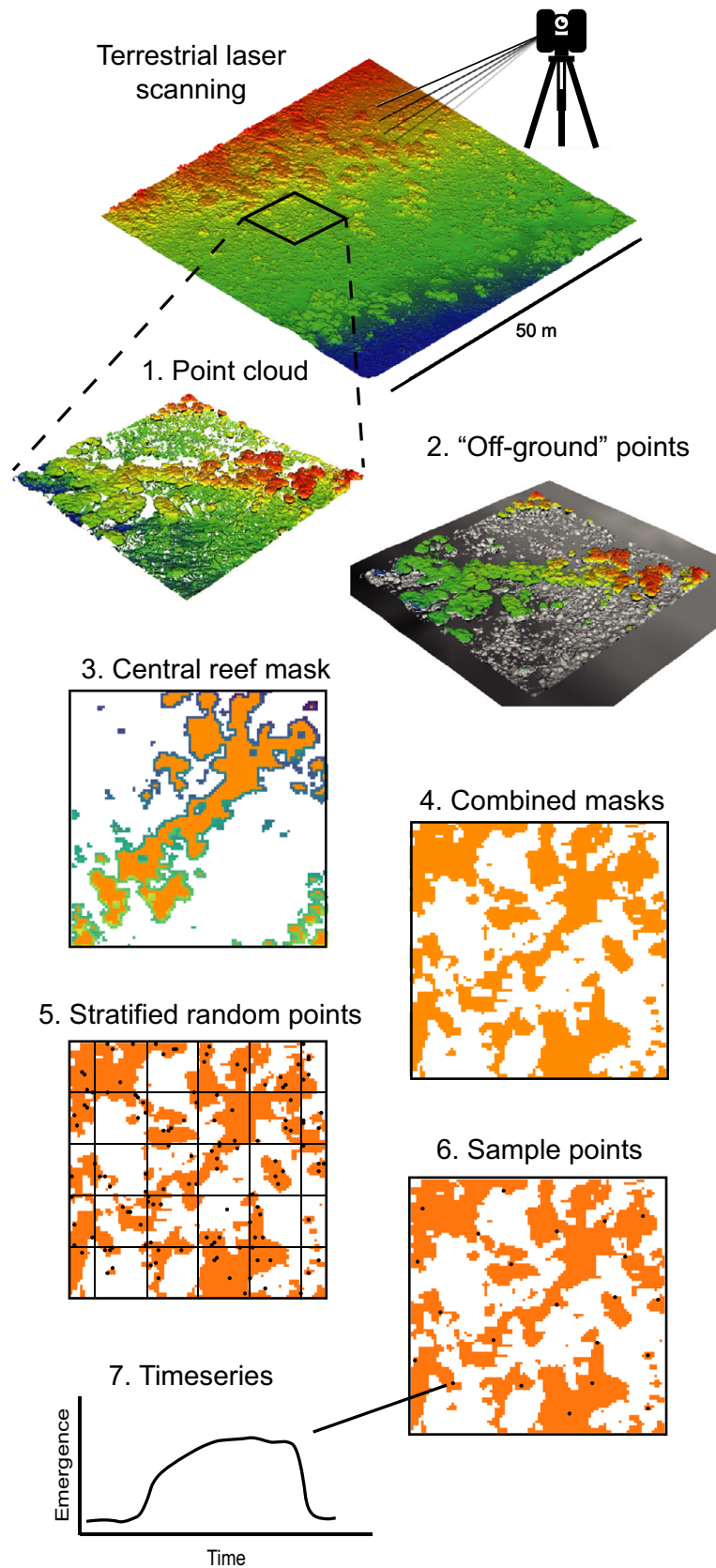


**Figure 4.** Data processing method used to sample reef emergence through time at independent reef locations within a 50 × 50 m plot mapped using terrestrial laser scanning at 6-month intervals over 5 years (Data S2). (1) Example section of 3D point cloud data. (2) We used a cloth simulation filter to generate a digital elevation model (DEM) for each time point and retained only points  $\geq 0.2$  m above the DEM. (3) We generated a digital surface model (DSM, 0.1 m XY resolution) of mean point elevation, then used the DSM to generate a mask that removed low point density cells, isolated cells, and colony edges. (4) We combined the masks from all time points. (5) We used a 2 m grid to generate spatially stratified random points (5 points per strata). (6) We randomly selected one point per strata with a minimum spacing of 1.5 m to generate our sample point locations. (7) At each sample location we calculated a timeseries of emergence by subtracting the elevation of a common DEM representing the ground level from the DSM for each time point (Fig. 7).

crucial step in understanding ecosystem dynamics and guiding their effective management. Here, for the first time, we quantified patterns of spatial and temporal variation in 3D habitat structure across scales in an ecologically important but understudied *Sabellaria alveolata* biogenic reef habitat. Our results reveal that patterns in reef emergence, accretion rate and erosion rate are spatially autocorrelated and highly scale dependent. In this system, reef colonies formed groups of rapidly accreting short-lived colonies and slow-accreting long-lived colonies, creating dynamic structure at fine spatial (m) and temporal (6 month) scales. However, these colony-scale dynamics cancel each other out at larger spatial (50 m to 1 km) and temporal (5 year) scales, resulting in seemingly stable reef habitat (Fig. 7). This habitat steady-state despite the mosaic of small-scale dynamics is akin to other biogenic systems like forests, where scale-dependent patterns in ecosystem properties have been better studied using remote sensing (Chambers et al., 2013). Using modern 3D mapping, we have quantified spatially continuous, cross-scale habitat structure in a biogenic reef, revealing scale-dependent patterns that indicate parallels in structural dynamics between terrestrial and marine biogenic habitats.

### Spatial patterns in reef habitat structure

We identified predictable trends in maximum reef emergence, accretion rate and erosion rate that all increased towards the lower shore. Shore height trends are ubiquitous in intertidal ecosystems like rocky shores and salt-marshes because numerous biological, chemical and physical structuring processes correlate with vertical position (Chappuis et al., 2014; Connell, 1972; Pennings & Callaway, 1992). The trends in our data can be explained by spatially varying hydrodynamic forces, proposed as the most important abiotic structuring factor of *S. alveolata* reef habitat (Collin et al., 2018; Gruet, 1986; Wilson, 1971). Wave forces are predicted to be greatest at the lower shore, with energy attenuated as waves travel across the rough reef surface (Bouma et al., 2014; Lowe et al., 2005). We suggest that higher wave energy at the lower shore results in more coarse sediment being resuspended

higher in the water column, enabling faster reef colony accretion and higher maximum emergence. Wave energy can also be destructive, increasing reef erosion rate towards the lower shore. In addition, longer periods of immersion experienced lower on the shore give more time for both reef accretion and erosion.

Interactions between individuals can produce spatially coherent self-organized patterns that influence ecosystem-scale processes in many natural systems, including mussel reefs (Van De Koppel et al., 2008) and arid vegetation (Klausmeier, 1999). We found evidence for self-organization in *S. alveolata* reef emergence and accretion rate that were spatially clustered (positively autocorrelated) up to colony scales (1.5 m). Prograding *S. alveolata* reef colonies have characteristic smooth surfaces comprising the openings of dense, parallel tubes (Fig. 1) (Curd et al., 2019; Ventura et al., 2020). To maintain this morphology as the colony grows, within-colony accretion rate and emergence must be similar among worms. Self-organization enhances habitat resilience (Guichard et al., 2003; Liu et al., 2014), and in this system the colony morphology may contribute to the remarkable wave resistance in the friable intertidal structures (Le Cam et al., 2011), analogous to massive stony coral morphologies that can dominate wave-exposed subtidal tropical reefs (Chappell, 1980).

Spatial patterns in biogenic reef properties provide insight into the biotic and abiotic drivers of ecosystem structuring processes (Aston et al., 2019; Edwards et al., 2017; Ford et al., 2020). In our system, reef emergence and accretion rates showed secondary spatial clustering at habitat scales (20–40 m down the shore, 110–130 m along the shore), whereas erosion rates showed spatial randomness beyond 4 m. Habitat-scale spatial clustering in reef emergence and accretion rate may be due to spatial variation in resources (e.g. sediment or food quality), environmental conditions (e.g. salinity), biotic factors (e.g. recruitment density) or anthropogenic influence (e.g. trampling). Interactions between myriad drivers are likely to influence reef structure at various scales (Collin et al., 2018). Identification of the relative importance of these factors and how they vary in time and space warrants further investigation, and may help explain why *S. alveolata*

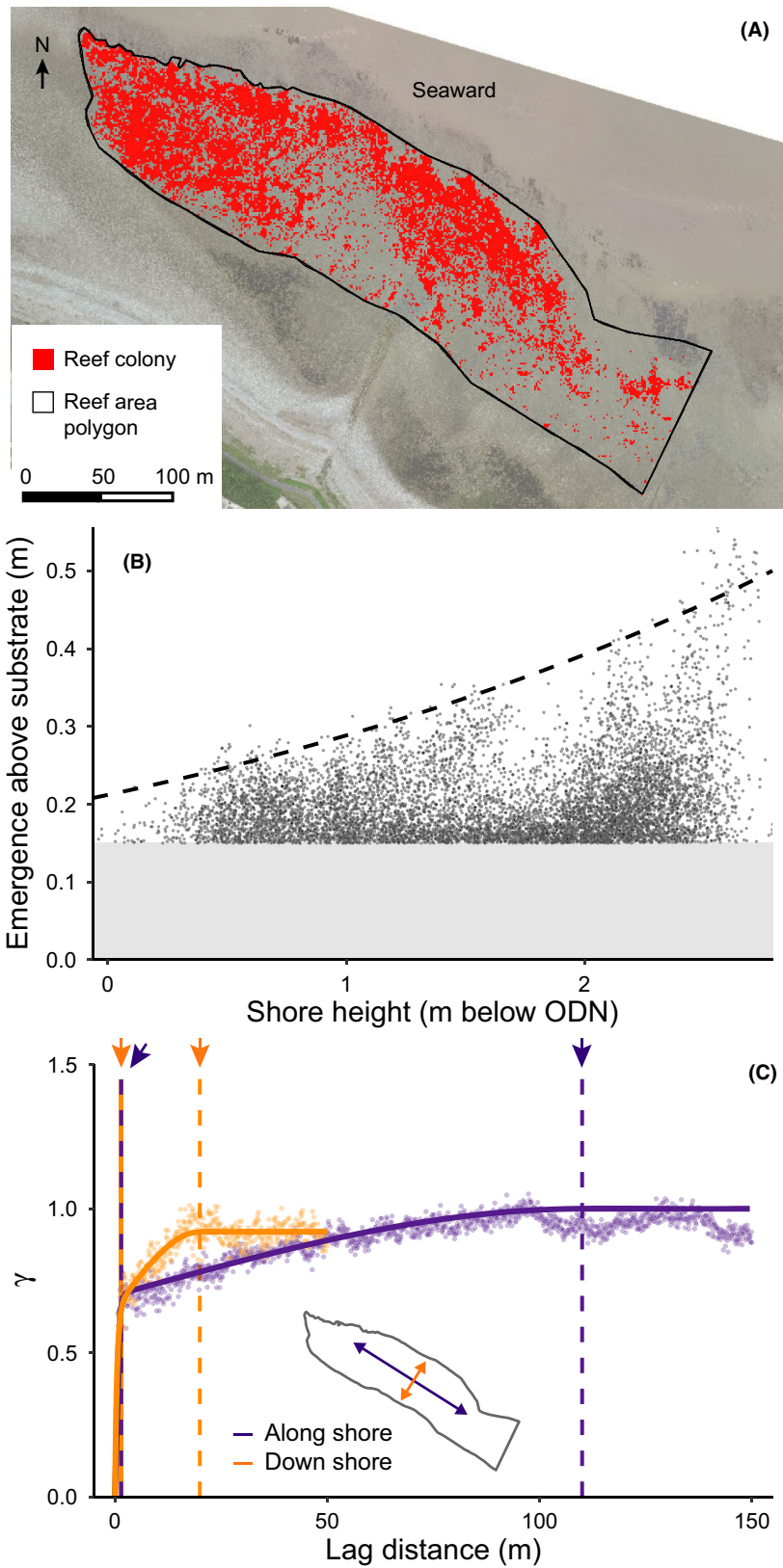
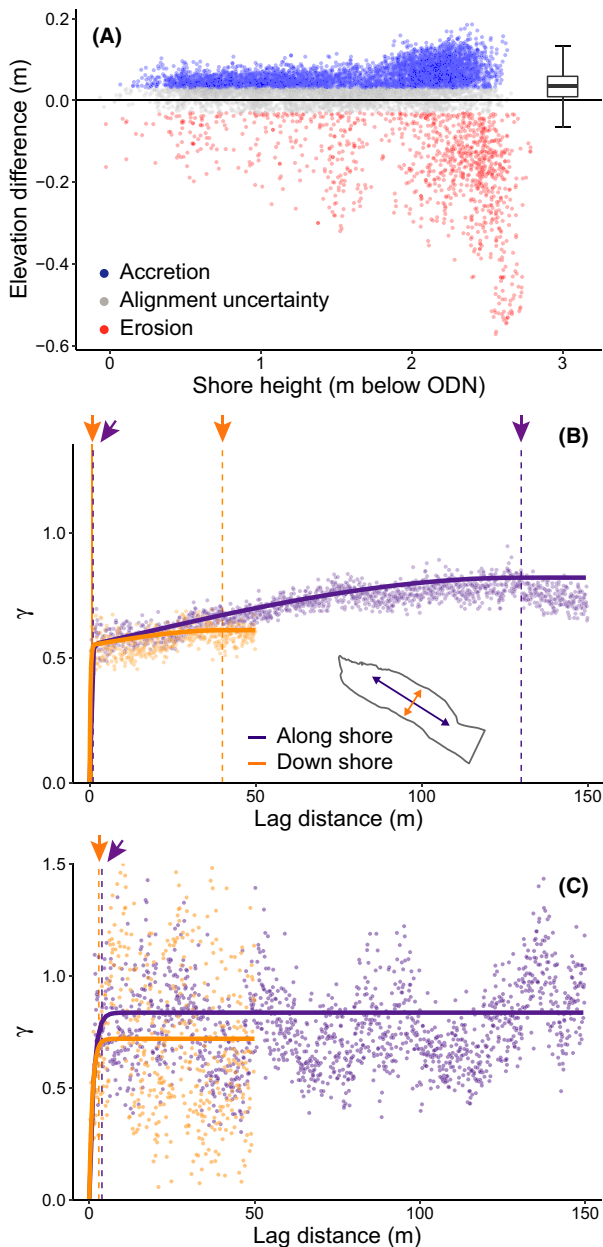


**Figure 5.** (A) The foreshore at Llanddulas, Wales, UK. Habitat-scale 3D structure data were analysed within a 36 363 m<sup>2</sup> reef area polygon digitized from an aerial imagery orthomosaic. Presence of emergent reef is shown at 1 m XY resolution. (B) Maximum reef colony emergence increases lower down the shore. The reef colonies that we analysed had a minimum emergence of 0.15 m. (C) Reef colony emergence was spatially autocorrelated over short distances (1.5 m) both along the shore (purple) and down the shore (orange), ranges indicated by left-most vertical lines and arrows. There was a secondary autocorrelation structure that had a longer range (110 m) in the along shore direction compared to down the shore (20 m), ranges shown by right-most vertical lines and arrows.

reef structure is highly variable among sites (Stone et al., 2019). Spatial clustering of erosion rates up to 4 m indicates that erosion mostly occurs as the catastrophic collapse of entire *S. alveolata* colonies and platform sections.



The lack of larger-scale spatial autocorrelation in erosion rates shows that colony collapse is random after accounting for shore height trends, suggesting that destructive processes are similar horizontally along the shore.

Modern remote-sensing technologies are advancing our ability to describe and interrogate spatial patterns in marine reef systems. In intertidal habitats like *S. alveolata* reef, aerial methods can capture a range of ecologically relevant information at high resolution across large extents of several km<sup>2</sup> (Bajjouk et al., 2020; Collin et al., 2018, 2019). The importance of 3D ecosystem structure in ecological investigations is recognized, and tools to capture and analyse 3D structure in diverse systems including subtidal reefs are becoming increasingly powerful and accessible (D'Urban Jackson et al., 2020; Lepczyk et al., 2021).

### Temporal patterns in biogenic reef structure

Identifying key scales of variation and their forcing processes has been a persistent challenge in ecology (Chave, 2013; Denny et al., 2004; Levin, 1992), especially in marine systems beyond the observation capabilities of traditional remote sensing (Lecours et al., 2015; Wedding et al., 2011). Our study reveals previously undescribed patterns of scale-dependent spatio-temporal variation in *S. alveolata* reef structure. We found that individual *S.*

**Figure 6.** Spatial variation in *S. alveolata* reef elevation changes from April 2018 to April 2019 within the reef area (Fig. 5A). (A) Both positive and negative elevation changes increased towards the lower shore. Samples showing positive changes (blue) were greater in number than those with negative change (red), but the larger average magnitude of negative changes resulted in little change in overall elevation, shown by the boxplot of all samples crossing 0. Grey points represent samples with changes within the alignment uncertainty estimate of  $\pm 0.03$  m. (B) Variogram showing spatial autocorrelation scales of positive elevation changes (accretion) after accounting for trend (Table S2). The majority of spatial autocorrelation is explained by a short range (0.75–1.05 m) structure (left-most vertical lines and arrows), with a secondary structure showing a longer range (130 m) in the alongshore orientation compared to down the shore (30 m). (C) Variogram showing spatial scales of negative elevation changes (erosion) after accounting for trend (Table S2). Spatial autocorrelation only occurs up to a short range (2.9–3.84 m, vertical lines and arrows).

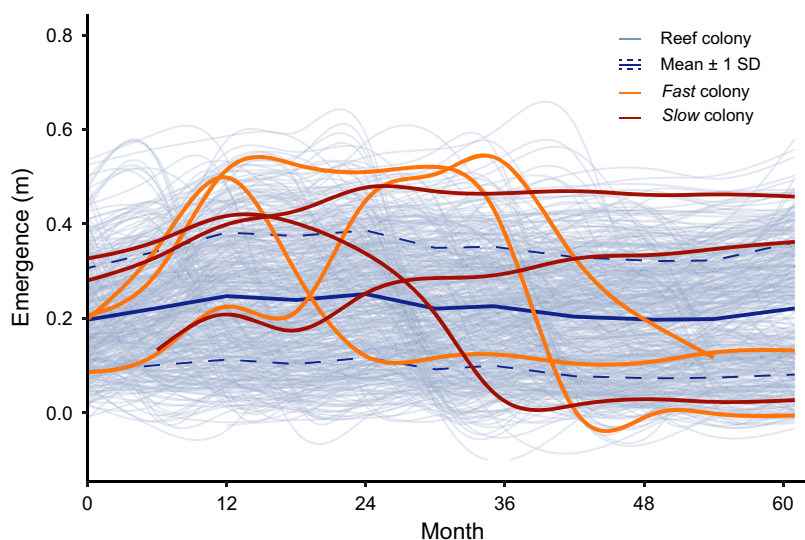


**Figure 7.** Colony-scale variation balances out to produce plot-scale stability in *S. alveolata* reef habitat structure over several years. Emergence was measured at 454 stratified random, spatially independent sample locations in a 2500 m<sup>2</sup> plot in autumn and spring each year from September 2014 (month 0) to October 2019 (month 61). Thin blue lines show individual sample timeseries. Bold blue line and dashed lines show the mean  $\pm$  1 sd emergence of all samples. Six example sample timeseries' are highlighted to show the diversity of fine-scale dynamics in reef accretion and loss over time, clustered into two groups: *fast* colonies with rapid accretion and short persistence (orange) and *slow* colonies with slower accretion and longer persistence (red).

*alveolata* colonies on the scale of metres undergo independent and compensatory accretion and erosion cycles, resulting in stability at larger spatial (2500 m<sup>2</sup>) and temporal (5 year) scales. Previous characterization of *S. alveolata* reef structural dynamics have described multiannual accretion and erosion cycles operating over large areas of reef (10 s to 100 s m) at some sites and multiannual stability at others (Gruet, 1986; Lecornu et al., 2016). While we recorded stability in reef structure over a period of 5 years, at decadal time scales, the habitat can be transient (Firth et al., 2015). Scale-dependent structural dynamism is a feature of other systems like terrestrial forests (Chambers et al., 2013), and our results indicate that conceptual frameworks from terrestrial landscape ecology can be applied to biogenic reef systems. For instance, the stability of a forest ecosystem can be modelled as a product of the spatial and temporal scales of disturbance events that it experiences (Turner et al., 1993). Applying this concept to our study system, disturbance events (colony collapse) were small in size (up to 4 m) relative to the habitat size (~35 000 m<sup>2</sup>) and disturbance (collapse) intervals were generally longer than recovery (accretion to maximum emergence) intervals. As predicted by the conceptual model (Turner et al., 1993), we observed stability in the system at the habitat scale.

We identified two distinct types of reef colonies: 'fast' colonies with rapid accretion, high maximum emergence and short lifespan, and 'slow' colonies with slower

accretion, lower maximum emergence and longer lifespan. Accretion rates of 'fast' *S. alveolata* colonies in our study (mean 0.109 m year<sup>-1</sup>, max 0.215 m year<sup>-1</sup>) were comparable to upper estimates of 0.105 m year<sup>-1</sup> in Cornwall, UK, and >0.5 m year<sup>-1</sup> in Normandy, France (Gruet, 1986; Wilson, 1971). These studies documented faster accretion rates in new, small colonies and a similar general pattern could be seen in our time series, although variation was high and many colonies had incomplete structural cycles within our study period. We found new, low emergent colonies accreted rapidly and then accretion slowed as they approached a maximum emergence, followed by a period of persistence at the maximum emergence and eventual rapid collapse. A similar accretion pattern has been documented in oyster (*Crassostrea virginica*) reefs, with rapid accretion in deeper edges of a reef (8 m diameter), while no change was recorded in the shallowest central portions, just 2 m away (Rodriguez et al., 2014). This fine-scale spatial variation in structural characteristics would be lost at larger observational scales, highlighting the need for a multi-scale approach when assessing the resilience of biogenic reefs to pressures like sea level rise.

Seasonal patterns of accretion and erosion in *S. alveolata* reef and their driving processes are not well understood. We did not find evidence for a consistent seasonal pattern in reef emergence, and while reef emergence measured in autumn showed some variation, spring

observations were stable over 5 years (Fig. S2, Table S4). However, we did find a seasonal difference in 1 survey year (2015). Temperature and wave energy are two dominant seasonally varying factors in intertidal habitats. The habitat is vulnerable to severe winter temperatures and damage from winter storms (Crisp, 1964; Firth et al., 2015). In summer, higher temperatures and increased food availability in summer may promote worm productivity that translates to increased accretion rate, but the availability of resuspended sediment with low summer wave action may limit accretion rate. Hydrodynamic energy promotes both *S. alveolata* reef accretion and erosion, so the effects of seasonal variation in wave energy are difficult to predict. Higher emergence in the autumn of 2015 compared to the spring appeared to be a result of heavy recruitment during the summer of that year (TDJ, *pers. obs.*), resulting in many new, rapidly accreting colonies. Recruitment of pelagic larvae to *S. alveolata* reefs is through a combination of continuous low-level settlement and stochastic heavy settlement events when hydrodynamic conditions are favourable (Ayata et al., 2009; Bush et al., 2015; Dubois et al., 2007). Sabellariidae worms respond to storm damage with increased reproductive output in a similar way that some plants respond to fire (Barry, 1989) and *S. alveolata* larvae show high levels of retention within local geographic areas (Bush et al., 2015; Dubois et al., 2007). These factors likely result in compensatory self-recruitment to a damaged reef, contributing to long-term reef persistence.

## Conclusion

Our findings represent the most comprehensive characterization of *S. alveolata* biogenic reef habitat structure across spatial and temporal scales to date, expanding our understanding of scale-dependent structural dynamics in this complex 3D habitat. We found that *S. alveolata* reef structure is characterized by a mosaic of different colony successional states leading to a dynamic landscape at smaller scales (m), while displaying relative stability (a steady state) at larger spatial and temporal scales. This phenomenon is characteristic of other structurally complex ecosystems like forests and we hypothesize that it could be true for other colonial reef systems, such as subtidal tropical coral reefs. We also identified previously undocumented temporal patterns in reef structure, specifically distinct groups of 'fast' and 'slow' colonies. The patterns we documented could only be detected with high-resolution 3D mapping, demonstrating the enhanced ecological insight gained from the adoption of contemporary technologies in modern ecology. Scale-dependent ecosystem patterns have historically been challenging to study due to necessary trade-offs in observation scale, especially

in marine systems. By embracing modern mapping technology in ecology, these long-standing constraints can be overcome, leading to an improved understanding of ecosystem dynamics in complex 3D habitats.

## Acknowledgments

This work formed part of the SEACAMS and SEACAMS2 projects, part funded by the European Regional Development Fund (ERDF) through the West Wales and the Valleys Programmes 2007–2013 and 2014–2020, with collaboration from Tidal Lagoon Power, Gloucester, GL2 5RG, UK. AJD was supported by the USDA National Institute of Food and Agriculture, Hatch Formula project accession number 1017848. Aerial imagery was provided under contract by OcuAir, Westbury, BA13 4JT, UK. We would like to thank Michael Roberts and Jonathan King for facilitating the study, and Laura Bush and Alex Vierød for their valuable insights. We thank two anonymous reviewers and Associate Editor Vincent Lecours for their valuable comments that improved the article.

## Author Contributions

All authors have seen and approved the submitted version of the manuscript. All authors have substantially contributed to the work, and all persons entitled to co-authorship have been included. TJB, AJD and GJW conceived and developed the study, TJB, GWS and SR collected the data, TJB processed and analysed the data and TJB, AJD and GJW wrote the manuscript. The manuscript has been submitted solely to *Remote Sensing in Ecology and Conservation* and it has not been published elsewhere, either in part or whole, or is it in press or under consideration for publication in another journal.

## Data Availability Statement

Data and R code supporting this manuscript are available in Figshare repositories, <https://doi.org/10.6084/m9.figshare.14480709> and <https://doi.org/10.6084/m9.figshare.14480703>.

## References

- Anderson, M.J. (2001) A new method for non-parametric multivariate analysis of variance. *Austral Ecology*, **26**, 32–46. <https://doi.org/10.1111/j.1442-9993.2001.01070.pp.x>
- Aston, E.A., Williams, G.J., Green, J.A.M., Davies, A.J., Wedding, L.M., Gove, J.M. et al. (2019) Scale-dependent spatial patterns in benthic communities around a tropical island seascape. *Ecography*, **42**(3), 578–590. <https://doi.org/10.1111/ecog.04097>

- Ayata, S.-D., Ellien, C., Dumas, F., Dubois, S. & Thiébaud, É. (2009) Modelling larval dispersal and settlement of the reef-building polychaete *Sabellaria alveolata*: role of hydroclimatic processes on the sustainability of biogenic reefs. *Continental Shelf Research*, **29**, 1605–1623. <https://doi.org/10.1016/j.csr.2009.05.002>
- Bajjouk, T., Jauzein, C., Drumetz, L., Dalla Mura, M., Duval, A. & Dubois, S.F. (2020) Hyperspectral and lidar: complementary tools to identify benthic features and assess the ecological status of *Sabellaria alveolata* reefs. *Frontiers in Marine Science*, **7**, 804. <https://doi.org/10.3389/fmars.2020.575218>
- Barry, J. (1989) Reproductive response of a marine annelid to winter storms: an analog to fire adaptation in plants? *Marine Ecology Progress Series*, **54**, 99–107. <https://doi.org/10.3354/meps054099>
- Bouma, T.J., van Belzen, J., Balke, T., Zhu, Z., Airoidi, L., Blight, A.J. et al. (2014) Identifying knowledge gaps hampering application of intertidal habitats in coastal protection: opportunities & steps to take. *Coastal Engineering*, **87**, 147–157. <https://doi.org/10.1016/j.coastaleng.2013.11.014>
- Bruschetti, M. (2019) Role of reef-building, ecosystem engineering polychaetes in shallow water ecosystems. *Diversity*, **11**, 168. <https://doi.org/10.3390/d11090168>
- Bush, L., Balestrini, S., Robins, P. & Davies, A. (2015) *NRW evidence report No 049 – The reproduction and connectivity of Sabellaria alveolata reefs in Wales – MAR4REF*. Bangor, UK: Natural Resources Wales.
- Calders, K., Phinn, S., Ferrari, R., Leon, J., Armston, J., Asner, G.P. et al. (2020) 3D imaging insights into forests and coral reefs. *Trends in Ecology & Evolution*, **35**, 6–9. <https://doi.org/10.1016/j.tree.2019.10.004>
- Capa, M., Hutchings, P. & Peart, R. (2012) Systematic revision of Sabellariidae (Polychaeta) and their relationships with other polychaetes using morphological and DNA sequence data. *Zoological Journal of the Linnean Society*, **164**, 245–284. <https://doi.org/10.1111/j.1096-3642.2011.00767.x>
- Chambers, J.Q., Asner, G.P., Morton, D.C., Anderson, L.O., Saatchi, S.S., Espírito-Santo, F.D.B. et al. (2007) Regional ecosystem structure and function: ecological insights from remote sensing of tropical forests. *Trends in Ecology & Evolution*, **22**, 414–423. <https://doi.org/10.1016/j.tree.2007.05.001>
- Chambers, J.Q., Negron-Juarez, R.L., Marra, D.M., Di Vittorio, A., Tews, J., Roberts, D. et al. (2013) The steady-state mosaic of disturbance and succession across an old-growth Central Amazon forest landscape. *Proceedings of the National Academy of Sciences*, **110**, 3949–3954. <https://doi.org/10.1073/pnas.1202894110>
- Chappell, J. (1980) Coral morphology, diversity and reef growth. *Nature*, **286**, 249–252. <https://doi.org/10.1038/286249a0>
- Chappuis, E., Terradas, M., Cefalù, M.E., Mariani, S. & Ballesteros, E. (2014) Vertical zonation is the main distribution pattern of littoral assemblages on rocky shores at a regional scale. *Estuarine, Coastal and Shelf Science*, **147**, 113–122. <https://doi.org/10.1016/j.ecss.2014.05.031>
- Chave, J. (2013) The problem of pattern and scale in ecology: what have we learned in 20 years? *Ecology Letters*, **16**, 4–16. <https://doi.org/10.1111/ele.12048>
- CloudCompare. (2019) *CloudCompare (version 2.11) [GPL software]*. Available at: <http://www.cloudcompare.org/>
- Collin, A., Dubois, S., James, D. & Houet, T. (2019) Improving intertidal reef mapping using UAV surface, red edge, and near-infrared data. *Drones*, **3**, 67. <https://doi.org/10.3390/drones3030067>
- Collin, A., Dubois, S., Ramambason, C. & Etienne, S. (2018) Very high-resolution mapping of emerging biogenic reefs using airborne optical imagery and neural network: the honeycomb worm (*Sabellaria alveolata*) case study. *International Journal of Remote Sensing*, **39**, 5660–5675. <https://doi.org/10.1080/01431161.2018.1484964>
- Connell, J.H. (1972) Community interactions on marine rocky intertidal shores. *Annual Review of Ecology and Systematics*, **3**, 169–192. <https://doi.org/10.1146/annurev.es.03.110172.001125>
- Connell, J.H. (1978) Diversity in tropical rain forests and coral reefs. *Science*, **199**, 1302–1310.
- Crisp, D.J. (1964) The effects of the severe winter of 1962–63 on marine life in Britain. *Journal of Animal Ecology*, **33**, 165. <https://doi.org/10.2307/2355>
- Curd, A., Pernet, F., Corporeau, C., Delisle, L., Firth, L.B., Nunes, F.L.D. et al. (2019) Connecting organic to mineral: how the physiological state of an ecosystem-engineer is linked to its habitat structure. *Ecological Indicators*, **98**, 49–60. <https://doi.org/10.1016/J.ECOLIND.2018.10.044>
- D'Urban Jackson, T., Williams, G.J., Walker-Springett, G. & Davies, A.J. (2020) Three-dimensional digital mapping of ecosystems: a new era in spatial ecology. *Proceedings of the Royal Society B-Biological Sciences*, **287**, 1–10. <https://doi.org/10.1098/rspb.2019.2383>
- Denny, M.W., Helmuth, B., Leonard, G.H., Harley, C.D.G., Hunt, L.J.H. & Nelson, E.K. (2004) Quantifying scale in ecology: lessons from a wave-swept shore. *Ecological Monographs*, **74**, 513–532. <https://doi.org/10.1890/03-4043>
- Dubois, S., Comtet, T., Retière, C. & Thiébaud, É. (2007) Distribution and retention of *Sabellaria alveolata* larvae (Polychaeta: Sabellariidae) in the Bay of Mont-Saint-Michel, France. *Marine Ecology Progress Series*, **346**, 243–254. <https://doi.org/10.3354/meps07011>
- Dubois, S., Retiere, C. & Olivier, F. (2002) Biodiversity associated with *Sabellaria alveolata* (Polychaeta: Sabellariidae) reefs: effects of human disturbances. *Journal of the Marine Biological Association of the United Kingdom*, **82**, 817–826. <https://doi.org/10.1017/S0025315402006185>

- Edwards, C.B., Eynaud, Y., Williams, G.J., Pedersen, N.E., Zgliczynski, B.J., Gleason, A.C.R. et al. (2017) Large-area imaging reveals biologically driven non-random spatial patterns of corals at a remote reef. *Coral Reefs*, **36**, 1291–1305. <https://doi.org/10.1007/s00338-017-1624-3>
- Firth, L.B., Mieszkowska, N., Grant, L.M., Bush, L.E., Davies, A.J., Frost, M.T. et al. (2015) Historical comparisons reveal multiple drivers of decadal change of an ecosystem engineer at the range edge. *Ecology and Evolution*, **5**, 3210–3222. <https://doi.org/10.1002/ece3.1556>
- Ford, H.V., Gove, J.M., Davies, A.J., Graham, N.A.J., Healey, J.R., Conklin, E.J. et al. (2020) Spatial scaling properties of coral reef benthic communities. *Ecography*, **44**(2), 188–198. <https://doi.org/10.1111/ecog.05331>
- Godet, L., Fournier, J., Jaffré, M. & Desroy, N. (2011) Influence of stability and fragmentation of a worm-reef on benthic macrofauna. *Estuarine, Coastal and Shelf Science*, **92**, 472–479. <https://doi.org/10.1016/j.ecss.2011.02.003>
- Graham, N.A.J., Jennings, S., MacNeil, M.A., Mouillot, D. & Wilson, S.K. (2015) Predicting climate-driven regime shifts versus rebound potential in coral reefs. *Nature*, **518**, 94–97. <https://doi.org/10.1038/nature14140>
- Graham, N.A.J. & Nash, K.L. (2013) The importance of structural complexity in coral reef ecosystems. *Coral Reefs*, **32**, 315–326. <https://doi.org/10.1007/s00338-012-0984-y>
- Graler, B., Pebesma, E. & Heuvelink, G. (2016) Spatio-temporal interpolation using gstat. *The R Journal*, **8**, 204–218.
- Gringarten, E. & Deutsch, C.V. (2001) Teacher's aide: variogram interpretation and modeling. *Mathematical Geology*, **33**, 507–534. <https://doi.org/10.1023/A:1011093014141>
- Gruet, Y. (1986) Spatio-temporal changes of Sabellarian reefs built by the sedentary polychaete *Sabellaria alveolata* (Linné). *Marine Ecology*, **7**, 303–319. <https://doi.org/10.1111/j.1439-0485.1986.tb00166.x>
- Guichard, F., Halpin, P.M., Allison, G.W., Lubchenco, J. & Menge, B.A. (2003) Mussel disturbance dynamics: signatures of oceanographic forcing from local interactions. *American Naturalist*, **161**, 889–904. <https://doi.org/10.1086/375300>
- Holt, T., Rees, E., Hawkins, S. & Seed, R. (1998) *Biogenic reefs (volume IX). An overview of dynamic and sensitivity characteristics for conservation management of marine SACs*. Oban, UK: Scottish Association for Marine Science (UK Marine SACs Project).
- Horne, J.K. & Schneider, D.C. (1995) Spatial variance in ecology. *Oikos*, **74**, 18. <https://doi.org/10.2307/3545670>
- Jenkins, C., Eggleton, J., Barry, J. & O'Connor, J. (2018) Advances in assessing *Sabellaria spinulosa* reefs for ongoing monitoring. *Ecology and Evolution*, **8**, 7673–7687. <https://doi.org/10.1002/ece3.4292>
- Jones, C.G., Lawton, J.H. & Shachak, M. (1994) Organisms as ecosystem engineers. *Oikos*, **69**, 373. <https://doi.org/10.2307/3545850>
- Kaiser, M.S., Speckman, P.L. & Jones, J.R. (1994) Statistical models for limiting nutrient relations in inland waters. *Journal of American Statistical Association*, **89**, 410–423. <https://doi.org/10.1080/01621459.1994.10476763>
- Kaufman, L. & Rousseeuw, P.J. (1990) *Finding groups in data, finding groups in data: an introduction to cluster analysis*, Wiley series in probability and statistics. Hoboken, NJ: John Wiley & Sons Inc. <https://doi.org/10.1002/9780470316801>
- Klausmeier, C.A. (1999) Regular and irregular patterns in semiarid vegetation. *Science*, **284**, 1826–1828. <https://doi.org/10.1126/science.284.5421.1826>
- Koenker, R. (2020) *Quantreg: quantile regression*. R package version 5.83. Available at: <https://CRAN.R-project.org/package=quantreg>
- La Porta, B. & Nicoletti, L. (2009) *Sabellaria alveolata* (Linnaeus) reefs in the central Tyrrhenian Sea (Italy) and associated polychaete fauna. *Zoosymposia*, **2**, 527–536. <https://doi.org/10.11646/zoosymposia.2.1.36>
- Landres, P.B., Morgan, P. & Swanson, F.J. (1999) Overview of the use of natural variability concepts in managing ecological systems. *Ecological Applications*, **9**, 1179–1188.
- Le Cam, J.-B., Fournier, J., Etienne, S. & Couden, J. (2011) The strength of biogenic sand reefs: visco-elastic behaviour of cement secreted by the tube building polychaete *Sabellaria alveolata*, Linnaeus, 1767. *Estuarine, Coastal and Shelf Science*, **91**, 333–339. <https://doi.org/10.1016/j.ecss.2010.10.036>
- Lecornu, B., Schlund, E., Basuyaux, O., Cantat, O. & Dauvin, J.-C.-C. (2016) Dynamics (from 2010–2011 to 2014) of *Sabellaria alveolata* reefs on the western coast of Cotentin (English Channel, France). *Regional Studies in Marine Science*, **8**, 157–169. <https://doi.org/10.1016/j.rsm.2016.07.004>
- Lecours, V., Devillers, R., Schneider, D.C., Lucieer, V.L., Brown, C.J. & Edinger, E.N. (2015) Spatial scale and geographic context in benthic habitat mapping: review and future directions. *Marine Ecology Progress Series*, **535**, 259–284. <https://doi.org/10.3354/meps11378>
- Legendre, P. & Fortin, M.J. (1989) Spatial pattern and ecological analysis. *Vegetatio*, **80**, 107–138. <https://doi.org/10.1007/BF00048036>
- Lepczyk, C.A., Wedding, L.M., Asner, G.P., Pittman, S.J., Goulden, T., Linderman, M.A. et al. (2021) Advancing landscape and seascape ecology from a 2D to a 3D science. *BioScience*. <https://doi.org/10.1093/biosci/biab001>
- Levin, S.A. (1992) The problem of pattern and scale in ecology: the Robert H. MacArthur Award Lecture author(s): Simon A. Levin source. *Ecology*, **73**, 1943–1967 <https://doi.org/10.2307/1941447>
- Liu, Q.-X., Herman, P.M.J., Mooij, W.M., Huisman, J., Scheffer, M., Olff, H. et al. (2014) Pattern formation at multiple spatial scales drives the resilience of mussel bed ecosystems. *Nature Communications*, **5**, 5234. <https://doi.org/10.1038/ncomms6234>

- Lowe, R.J., Falter, J.L., Bandet, M.D., Pawlak, G., Atkinson, M.J., Monismith, S.G. et al. (2005) Spectral wave dissipation over a barrier reef. *Journal of Geophysical Research*, **110**, 1–16. <https://doi.org/10.1029/2004JC002711>
- Maechler, M., Rousseeuw, P.J., Struyf, A., Hubert, M. & Hornik, K. (2019) *Cluster: cluster analysis basics and extensions*. R package version 2.1.0.
- Odum, E.P. (1969) The strategy of ecosystem development. *Science*, **164**, 262–270.
- Pebesma, E.J. (2004) Multivariable geostatistics in {S}: the gstat package. *Computers & Geosciences*, **30**, 683–691.
- Pennings, S.C. & Callaway, R.M. (1992) Salt marsh plant zonation: the relative importance of competition and physical factors. *Ecology*, **73**, 681–690. <https://doi.org/10.2307/1940774>
- Perry, G.L.W. (2002) Landscapes, space and equilibrium: shifting viewpoints. *Progress in Physical Geography*, **26**, 339–359. <https://doi.org/10.1191/0309133302pp341ra>
- Peterson, R.A. & Cavanaugh, J.E. (2020) Ordered quantile normalization: a semiparametric transformation built for the cross-validation era. *Journal of Applied Statistics*, **47**, 2312–2327. <https://doi.org/10.1080/02664763.2019.1630372>
- R Core Team. (2020) *R: a language and environment for statistical computing*. Vienna, Austria: R Foundation for Statistical Computing Available at: <https://www.R-project.org/>
- Rodriguez, A.B., Fodrie, F.J., Ridge, J.T., Lindquist, N.L., Theuerkauf, E.J., Coleman, S.E. et al. (2014) Oyster reefs can outpace sea-level rise. *Nature Climate Change*, **4**, 493–497. <https://doi.org/10.1038/nclimate2216>
- Safriel, U.N. & Ben-Eliahu, M.N. (1991) The influence of habitat structure and environmental stability on the species diversity of polychaetes in vermetid reefs. In: Bell, S.S., McCoy, E.D. & Mushinsky, H.R. (Eds.) *Habitat structure*. London: Chapman & Hall/CRC, pp. 349–368. <https://doi.org/10.1007/978-94-011-3076-9>
- Scheffers, B.R., Edwards, D.P., Diesmos, A., Williams, S.E. & Evans, T.A. (2014) Microhabitats reduce animal's exposure to climate extremes. *Global Change Biology*, **20**, 495–503. <https://doi.org/10.1111/gcb.12439>
- Stevenson, A., Mitchell, F.J.G. & Davies, J.S. (2015) Predation has no competition: factors influencing space and resource use by echinoids in deep-sea coral habitats, as evidenced by continuous video transects. *Marine Ecology*, **36**, 1454–1467. <https://doi.org/10.1111/maec.12245>
- Stone, R., Callaway, R. & Bull, J.C. (2019) Are biodiversity offsetting targets of ecological equivalence feasible for biogenic reef habitats? *Ocean & Coastal Management*, **177**, 97–111. <https://doi.org/10.1016/j.ocecoaman.2019.04.003>
- Turner, M.G., Romme, W.H., Gardner, R.H., O'Neill, R.V. & Kratz, T.K. (1993) A revised concept of landscape equilibrium: disturbance and stability on scaled landscapes. *Landscape Ecology*, **8**, 213–227. <https://doi.org/10.1007/BF00125352>
- Underwood, A.J., Chapman, M.G. & Connell, S.D. (2000) Observations in ecology: you can't make progress on processes without understanding the patterns. *Journal of Experimental Marine Biology and Ecology*, **250**, 97–115. [https://doi.org/10.1016/S0022-0981\(00\)00181-7](https://doi.org/10.1016/S0022-0981(00)00181-7)
- Urbina-Barreto, I., Chiroleu, F., Pinel, R., Fréchon, L., Mahamadaly, V., Elise, S. et al. (2021) Quantifying the shelter capacity of coral reefs using photogrammetric 3D modeling: from colonies to reefscales. *Ecological Indicators*, **121**, 107151. <https://doi.org/10.1016/j.ecolind.2020.107151>
- Van De Koppel, J., Gascoigne, J.C., Theraulaz, G., Rietkerk, M., Mooij, W.M. & Herman, P.M.J. (2008) Experimental evidence for spatial self-organization and its emergent effects in mussel bed ecosystems. *Science*, **322**, 739–742. <https://doi.org/10.1126/science.1163952>
- Ventura, D., Dubois, S.F., Bonifazi, A., Jona Lasinio, G., Seminara, M., Gravina, M.F. et al. (2020) Integration of close-range underwater photogrammetry with inspection and mesh processing software: a novel approach for quantifying ecological dynamics of temperate biogenic reefs. *Remote Sensing in Ecology and Conservation*. <https://doi.org/10.1002/rse2.178>
- Vierling, K.T., Vierling, L.A., Gould, W.A., Martinuzzi, S. & Clawges, R.M. (2008) Lidar: shedding new light on habitat characterization and modeling. *Frontiers in Ecology and the Environment*, **6**, 90–98. <https://doi.org/10.1890/070001>
- Warfe, D.M., Barmuta, L.A. & Wotherspoon, S. (2008) Quantifying habitat structure: surface convolution and living space for species in complex environments. *Oikos*, **117**, 1764–1773. <https://doi.org/10.1111/j.1600-0706.2008.16836.x>
- Wedding, L.M., Jorgensen, S., Lepczyk, C.A. & Friedlander, A.M. (2019) Remote sensing of three-dimensional coral reef structure enhances predictive modeling of fish assemblages. *Remote Sensing in Ecology and Conservation*, **5**, 150–159. <https://doi.org/10.1002/rse2.115>
- Wedding, L., Lepczyk, C., Pittman, S., Friedlander, A. & Jorgensen, S. (2011) Quantifying seascape structure: extending terrestrial spatial pattern metrics to the marine realm. *Marine Ecology Progress Series*, **427**, 219–232. <https://doi.org/10.3354/meps09119>
- Wiens, J.A. (1989) Spatial scaling in ecology. *Functional Ecology*, **3**, 385. <https://doi.org/10.2307/2389612>
- Williams, G.J., Graham, N.A.J., Jouffray, J.B., Norström, A.V., Nyström, M., Gove, J.M. et al. (2019) Coral reef ecology in the Anthropocene. *Functional Ecology*, **33**, 1014–1022. <https://doi.org/10.1111/1365-2435.13290>
- Wilson, D.P. (1971) Sabellaria colonies at Duckpool, North Cornwall. *Journal of the Marine Biological Association of the United Kingdom*, **51**, 509–580.
- Woodhead, A.J., Hicks, C.C., Norström, A.V., Williams, G.J. & Graham, N.A.J. (2019) Coral reef ecosystem services in the Anthropocene. *Functional Ecology*, **33**, 1023–1034. <https://doi.org/10.1111/1365-2435.13331>

## Supporting Information

Additional supporting information may be found online in the Supporting Information section at the end of the article.

**Data S1.** Analysis of spatial patterns and scales of variation using variography.

**Dats S2.** Sampling reef emergence through time at the 2,500m<sup>2</sup> plot scale.

**Figure S1.** 2500 m<sup>2</sup> plot showing 0.01 m<sup>2</sup> cells containing *S. alveolata* reef in at least one of 11 surveys over 5 years (grey) and stratified random, spatially independent samples (crosses).

**Figure S2.** Boxplot of emergence within the 2500 m<sup>2</sup> plot surveyed using terrestrial laser scanning at approximately

6 month intervals over 5 years, with median (bar) and mean (open circles) displayed.

**Table S1.** Spatial structure parameters of reef and substrate emergence within the ~35 000 m<sup>2</sup> reef area, derived from variography.

**Table S2.** Spatial structure parameters of reef accretion (positive elevation change) and erosion (negative elevation change) within the ~35 000 m<sup>2</sup> reef area over one year, derived from variography.

**Table S3.** Average accretion and erosion metrics for two groups of reef colonies identified within the 2500 m<sup>2</sup> plot.

**Table S4.** Results of permutational analysis of variance, testing for the effects of year, season and their interaction on emergence within the 2500 m<sup>2</sup> plot.